Ann Oper Res
DOI 10.1007/s10479-017-2581-5

Obstacle-aware optimization of offshore wind farm cable layouts

Arne Klein[1] · **Dag Haugland**[1]

Abstract In this article, an integer linear programming model for cost minimization of cable layouts in offshore wind farms is presented. All turbines must be connected to power substations by cables. Up to a given number, turbines may be connected along a joint cable in a series circuit, and cable branching at turbine locations is possible. No two cables are allowed to cross each other. As an improvement over previously available models, the model under study enables optimal adaptation of the cable routes to obstacles. Obstacles of two different kinds are considered. First, a set of regions in which cables cannot be laid is accepted as part of the input to the model. Second, the trajectory of one cable plays the role of an obstacle to all other cables. Both obstacle types are modeled by introducing optional connection points, which, contrary to the turbines, do not have to be visited by any cable. By introducing such optional connection points at selected positions, we arrive at a model with some resemblance with the Steiner tree problem. We demonstrate that, by virtue of the optional points, the suggested model is able to identify feasible solutions to problem instances where other models fail to do so. In other instances, the model yields more cost-effective cable layouts than previously studied models do. Computational experiments with realistic wind farm instances of up to 88 turbines prove that cabling cost reductions of about 1% are achievable by the model.

Keywords Integer programming model · Offshore wind farm · Cable layout · Obstacle avoidance · Computational experiments

1 Introduction

Offshore wind energy is becoming an increasingly more important energy source, and is one of the fastest growing energy sectors. Up to now, the main development is taking place in

✉ Dag Haugland
dag.haugland@ii.uib.no

Arne Klein
arne.klein@ii.uib.no

[1] Department of Informatics, University of Bergen, Bergen, Norway

Published online: 24 July 2017

Northern Europe, with 6562 MW out of the global installed capacity of 7045 MW installed in Europe at the end of 2013 (GWEC 2015). By far, the most important countries in this respect are the United Kingdom and Denmark, with PR China, Belgium, Germany, Netherlands and Sweden following. Installed capacity in other countries is of negligible size.

Commercial offshore wind energy started in Europe in the year 2000 with an installed capacity of only 4 MW. The total installed capacity in Europe as of the end of 2016 is 12.6 GW (WindEurope 2017). A record annual installation of 3000 MW took place in 2015, almost twice as much as in any other year. It is estimated that the installed capacity grows to 24.6 GW by 2020 (WindEurope 2017).

The largest offshore wind farm in operation is London Array (London Array Limited 2017), with 175 turbines and a total installed capacity of 400 MW. The average size of grid-connected offshore wind farms in Europe by the end of 2016 is however only 156 MW with 44 turbines. Offshore wind farm size is steadily increasing, with the farms under construction in 2016 having an average of 380 and 4.8 MW per turbine, resulting in an average of 77 turbines (WindEurope 2017). Large wind farms with over 150 turbines are no longer uncommon for offshore wind farms under construction or in the planning phase, as for example the Hornsea One project, with an expected 1.2 GW installed capacity (WindEurope 2017) and 174 turbines (DONG 2017).

There are three main applications of operations research in the planning and operation of offshore wind farms. The first category consists of a large number of contributions with their focus on operations and maintenance (Irawan et al. 2017). This often includes fleet and possibly personnel planning, taking into account expected life times of components, required maintenance intervals, weather and more. Another application of operations research is the short-term forecasting of wind power generation (Foley et al. 2012). The third operations research application is the layout planning of wind farms, including turbine, electric substation and cable locations in such a way that the expected net income is maximized, possibly taking into account expected maintenance costs (Réthoré et al. 2014). In the following we limit the literature review on computing optimal cable paths, which is the topic of the current work.

During the planning and construction phase of an offshore wind farm, the cabling routes can often be chosen freely, possibly with some obstacles to consider. Each turbine needs to be connected to a power substation, from which the energy is transferred to an onshore location. Multiple turbines can be connected by one cable in a series circuit. The maximum number of turbines on one cable depends on the cable type. Currently installed wind farms often have a maximum of four to eight turbines per cable. Additional constraints on the cable paths may apply. A typical limitation is that intersections of cables are not allowed, as this interferes with the trenching process.

As the cable and trenching costs per meter are significant, it is crucial for the wind farm operator to bring the total cabling costs to a minimum. To this end, optimization techniques tailored to determine the cable paths can be extremely useful.

Early works on optimizing cable layouts mainly use metaheuristic approaches. Genetic algorithms are, for example, used by Lingling et al. (2009) and Gonzalez-Longatt et al. (2012). Recently, by use of integer linear programming models, exact methods have become more prevalent.

Optimization of cable routes in offshore wind farms is addressed by Bauer and Lysgaard (2015), who introduce a model with hop-indexed variables, resembling a planar open vehicle routing problem. Respecting that cables are not allowed to cross each other, planarity constraints apply to the model. For a given cable capacity, as well as fixed turbine and substation

locations, the objective of the model by Bauer and Lysgaard (2015) is to find the cable routes of minimum total length.

An important assumption of Bauer and Lysgaard (2015) is that the turbines are connected to substations along paths. That is, with the exceptions of the turbine closest to and most remotely from the substation, all turbines have a direct link with exactly two other turbines. In several practical cases, however, it is possible to branch the power cables at the turbine locations without significant additional effort or cost. Such options offer opportunities for further reductions of the total required cable length, and thereby the total costs. Branched cables are already implemented in some existing wind farms. This includes, for example, the Walney 1 offshore wind farm, which is located on the Northwestern English coast. Improved models accounting for the option to branch cables at turbine locations have been presented in several publications, including Pillai et al. (2015), Klein et al. (2015) and Wdzik et al. (2016).

The publication by Pillai et al. (2015) also introduces a possible way of dealing with *obstacles* obstructing the cable paths. They introduce a pre-processing step that calculates the shortest valid path between turbine locations, which is in turn used as the edge cost in the optimization process. Fischetti and Pisinger (2016) present a different approach of dealing with obstacles. By introducing Steiner points at the corners, it becomes possible to compute paths for single cables around obstacles. A mixed integer linear programming model, as well as a heuristic approach, are discussed.

Obstacles can exist due to geologic features of the sea bed, governmental regulations, environmental protection, or other reasons. Further, cables with a completely different purpose than serving the wind farm, may already be installed in its region. Examples of obstacles restricting the possible choices of cable paths for connecting the turbines can be found in several offshore wind farms. The Walney 2 offshore wind farm is crossed by a subsea telecommunications cable, and West of Duddon Sands by methanol, gas, and power pipelines (KIS-ORCA 2017). The sandbanks Inner Gabbard and The Galloper are in the center of the Greater Gabbard project. Those are Special Areas of Conservation, and each of them is only intersected at one location by cables (Greater Gabbard Offshore Winds Ltd 2005).

Over the past few years, a number of research articles on optimized cable routes have emerged. Cerveira et al. (2016) focus on a detailed energy loss modelling, resulting in an integer linear programming formulation minimizing the costs of infrastructure and energy losses. A similar focus is applied by Wdzik et al. (2016), accounting for trenching and energy loss costs, in addition to cable costs. Cable crossings are not disallowed in this work. The cable cross-section is optimized simultaneously with the cable layout, which is done in a more abstract way by Klein et al. (2015). Hou et al. (2016) develop a dynamic minimum spanning tree algorithm for solving the cable layout problem. allowing for cables to be laid in parallel. Hertz et al. (2017) propose a mixed integer linearized quadratic programme to optimize the cable layout with different cable types available.

Apart from Pillai et al. (2015) and Fischetti and Pisinger (2016), none of the works cited here take obstacles into account. In this article, we suggest a model which introduces *optional cable connection points* in addition to the mandatory turbine connection points, with similarities to Fischetti and Pisinger (2016). Such an approach leads to a network model resembling the well-studied *minimum Steiner tree model* (Hwang et al. 1992), which aims to find a tree of minimum cost connecting all *terminal* nodes of a graph, with optional use of *Steiner* nodes. Turbine locations play the role of terminals in this context, while optional connection points at the boundary of obstacles are examples of Steiner nodes.

Representing polygonal obstacles by means of Steiner nodes located at their vertices, introduces an approach that goes beyond the one taken by Pillai et al. (2015). Because of

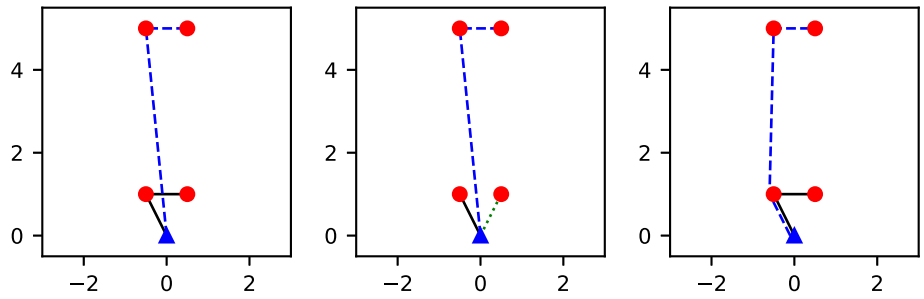

Fig. 1 Wind farm where the optimal cable routes have a parallel section

constraints saying that two cable routes are not supposed to cross, it is in some cases non-optimal to lay the cable along the shortest path around an obstacle. When more than one path around an obstacle are available, presence of Steiner nodes enables optimization of the choice of a cable path, while taking into account the non-crossing constraints with other cables.

Owing to the non-crossing constraints, the route of one cable is an hindrance to other cables. Optimal adaption to such obstructions can also be accomplished by means of Steiner nodes. Letting the turbine locations be surrounded by Steiner nodes allows two or more cables to run in parallel, in a shared trench, along a section of their routes. Each turbine along such parallel route sections is connected to the grid via exactly one of the present cables. It is easily demonstrated that cost reductions thus are achievable, even in wind farms without obstacles of a physical or legal nature. Models that do not acknowledge Steiner nodes are likely to miss these reductions, as they deem infeasible the corresponding cable layout.

An example of an instance where parallel cable routes are optimal is illustrated in Fig. 1. In this example, the cable capacity is 2, meaning that each cable cannot connect more than 2 turbines. A turbine is located at each red circular dot, and a substation to which the turbines must be connected, is located at the blue triangle. Different cables are indicated by the black solid, blue dashed and green dotted lines. The same color, shape and line-coding are used in all following illustrating figures. An infeasible solution, violating the non-crossing constraint, is shown on the left (cable cost = cable length = 8.14). The solution defined optimal by models that do not include Steiner nodes and the parallel cable option is shown in the middle (cable length = 8.26). Finally, the optimal solution identified by a model featuring parallel cables is given on the right (cable length 8.24). The cable corresponding to the black line connects the southwestern (and the southeastern) turbine to the substation, whereas the other cable (blue line), hindered by the first cable, takes advantage of a Steiner node located by the southwestern turbine.

The remainder of this text is organized as follows: In the next section, we describe in detail the problem to be solved. We follow this up by giving the model definition in Sect. 3. After introducing model and notation, we continue in Sect. 4.3 with a presentation of the numerical results obtained from an implementation of our model.

2 Problem definition

This section starts with a description of the cable layout problem from an engineering point of view. Next, we introduce mathematical notation and definitions used throughout the article, before we give a concise problem definition in mathematical terms.

2.1 The cable layout optimization problem

We assume that the turbine layout of an offshore wind farm is given, including the location of all turbines and power substations. On which parts of the seabed it is possible to lay cables has also been assessed.

Each turbine needs to be connected to exactly one substation by a cable. Multiple turbines can be connected to a power substation by the same cable in a series circuit. Ramified connections are considered, as the cables are allowed to branch at turbine locations.

Following the model by Klein et al. (2015), there is an upper bound, referred to as the *cable capacity*, on the maximum number of turbines connected to the same cable. Due to practical limitations, there is also an upper bound on the number of branches a cable can make at a turbine location. We refer to this bound as the *branching capacity*. Contrasting Klein et al. (2015), we consider a unique cable type. Connecting a turbine directly to another turbine or to a substation incurs a cost, which depends on the distance between the two connection points. For simplicity, we assume that the cost is proportional to the distance, such that minimizing total cable costs becomes equivalent to minimizing the sum of all cable lengths.

It is possible to lay several cables in parallel, and arbitrarily close to each other, e.g. in a shared trench. Different cables can thus partly follow a common trajectory, such that some turbines are visited by more than one cable. Only one visiting cable is connected to the turbine. Parallel cables can represent a cost-saving measure, especially by means of avoiding *crossing cables*. Owing to technical limitations in the trenching process, cables crossing each other are disallowed. As discussed in Sect. 1, and demonstrated in Fig. 1, such restrictions imply in many instances that the optimal solution has sections of parallel cables.

The non-crossing restriction applies also to cables that partly run in parallel. Consider, for example, two cables next to each other following partly a straight line directed from north to south. Then, the cable entering the joint trajectory from the westernmost position also has to leave in the westernmost direction. More generally, parallel cables are allowed if they can be drawn as two lines arbitrarily close to the joint trajectory, but in such a way that the lines nowhere intersect. This condition represents a considerable modelling challenge receiving extensive attention in the current work.

Not all parts of the sea bed are available for cable laying. We consider a set of such *obstacles*, the interior of which none of the cables are allowed to intersect. Pillai et al. (2015) suggest to deal with the obstacles in a preprocessing procedure, which, for all pairs of turbines, computes the length of the shortest feasible trajectory connecting them. Such an approach has the advantage that the lengths of all turbine-to-turbine connection links are known, and can be provided as input to an optimization model. However, it relies on prior knowledge to what trajectory around an obstacle will be chosen, and confines the choice to the shortest route. More flexibility, especially with respect to crossing conflicts with other cables, is obtained if also the obstacle avoidance route is optimized.

To that end, we introduce *optional connection points*. We assume that each obstacle is defined in terms of a *convex polygon*. Although more general obstacle geometries certainly are observable in practice, the assumption is rather mild. Areas inside the convex hull of a non-convex obstacle are unlikely to be attractive connection points, and it is thus reasonable to extend the obstacle to its convex hull. Further, non-polyhedral obstacles can be closely approximated by enclosing convex polygons. For each polygon in question, we let all its vertices be optional connection points. All direct cable links are assumed to be rectilinear, and direct links intersecting some obstacle interior are disallowed.

The aim is to find a set of cable routes respecting the above conditions, such that all turbines are connected to a substation via a cable, and such that the total costs are minimized.

We now go on to define this problem in precise mathematical terms, which later (Sect. 3) is developed into an integer programming model.

2.2 Abstract problem definition

Let $G = (N, A)$ be a directed graph with node set N and arc set A. The nodes are partitioned into subsets T, D and O, where nodes in $T \subset N$ correspond to the turbines, and are henceforth referred to as *turbine nodes*. Analogously, the *substation nodes* in D correspond to substations. Finally, the *obstacle nodes* in O correspond to the optional connection points located at obstacle vertices.

The arc set consists of all pairs of nodes corresponding to turbines, substations or optional connection points that can be connected directly with a rectilinear cable link. Applying the convention that connections are directed *towards substations*, the arc set satisfies $A \subseteq (T \cup O) \times N$, meaning that no arcs in A leave a substation node. The containment is satisfied by equality if there are no obstacles to consider.

The notation $H \subseteq G$ means that H is a subgraph of G, with node set denoted $N(H) \subseteq N$ and arc set denoted $A(H) \subseteq A$, where $(i, j) \in A(H)$ implies $i, j \in N(H)$. We let δ^+_{iH} and δ^-_{iH} denote, respectively, the out-degree and the in-degree of node $i \in N(H)$ in subgraph H.

The function $L : N \mapsto \mathbb{R}^2$ defines the *embedding* of the nodes in the plane. The embedding of arc $(i, j) \in A$ is the closed line segment from $L(i)$ to $(L(j)$, denoted $L(i, j) = \{L(i) + \lambda(L(j) - L(i)) : \lambda \in [0, 1]\}$. Further, the embedding of $H \subseteq G$ is defined as the set $L(H) = \bigcup_{(i,j)\in A(H)} L(i, j)$.

We refer to the function $c : A \mapsto \mathbb{R}_+$ as the *arc cost*, and let $c(i, j) = \|L(i) - L(j)\|_2$ be the Euclidean distance between $L(i)$ and $L(j)$. Hence, c fulfills the triangle inequality $c(i, k) \leq c(i, j) + c(j, k)$ for arcs $(i, k), (i, j), (j, k) \in A$. We also define the positive integers C and m, denoting, respectively, the cable and branching capacities.

For all $\mathbf{x} \in \mathbb{R}^2$ and closed sets $\mathbf{X} \subseteq \mathbb{R}^2$, we define $\text{dist}(\mathbf{x}, \mathbf{X}) = \min_{\widehat{\mathbf{x}}\in\mathbf{X}} \|\widehat{\mathbf{x}} - \mathbf{x}\|_2$. We let $\partial\mathbf{X}$ denote the set of boundary points of $\mathbf{X}$. For points $\mathbf{x}_1, \mathbf{x}_2 \in \mathbb{R}^2$, $[\mathbf{x}_1, \mathbf{x}_2]$ denotes the closed line segment with end points $\mathbf{x}_1$ and $\mathbf{x}_2$. For $i, j, k \in N$, where $i \neq j \neq k \neq i$,

$$\text{cone}(i, j, k) = \left\{\mathbf{x} \in \mathbb{R}^2 : \mathbf{x} = L(j) + \lambda_i\,(L(i) - L(j)) + \lambda_k\,(L(k) - L(j)) : \lambda_i, \lambda_k \geq 0\right\}$$

denotes the translation of the *conical hull* of $L(i) - L(j)$ and $L(k) - L(j)$, such that the origin is translated to $L(j)$.

In the following, we let $\mathcal{H}$ denote a set of directed trees in G.

Definition 1 The set $\mathcal{H}$ is *crossing-free* if, for all $\varepsilon > 0$, there exists a function $F_H : L(H) \mapsto \mathbb{R}^2$ for each $H \in \mathcal{H}$, such that (let $F_H(L(H))$ denote the image of F_H)

1. $\|F_H(L(n)) - L(n)\|_2 \leq \varepsilon$ for all $H \in \mathcal{H}$ and all $n \in N(H)$,
2. $F_H(L(H)) \cap F_{H'}\left(L(H')\right) = \varnothing$ for all $H, H' \in \mathcal{H}$, $H \neq H'$, and
3. $F_H\left(L(i, j)\right) \cap F_H\left(L(i', j')\right) \subset F_H\left(\{L(i), L(j), L(i'), L(j')\}\right)$ for all $H \in \mathcal{H}$ and all $(i, j), (i', j') \in A(H)$.

Remark 1 Condition 1 states that the perturbation function F_H moves each point in $L(H)$ no more than ε units from its original position. Condition 2 states that when applying all perturbation functions to their respective tree embeddings, all pairs of trees have disjoint embeddings. Finally, condition 3 states that after perturbation, the embeddings of two arcs in H intersect only at their endpoints.

Remark 2 If $(i, j) \in A(H)$, $(i', j') \in A(H')$, and $H, H' \in \mathcal{H}$, where arcs (i, j) and (i', j') cross in the sense that $L(i, j) \cap L(i', j') \setminus \{L(i), L(j), L(i'), L(j')\} \neq \varnothing$, then $\mathcal{H}$ is not

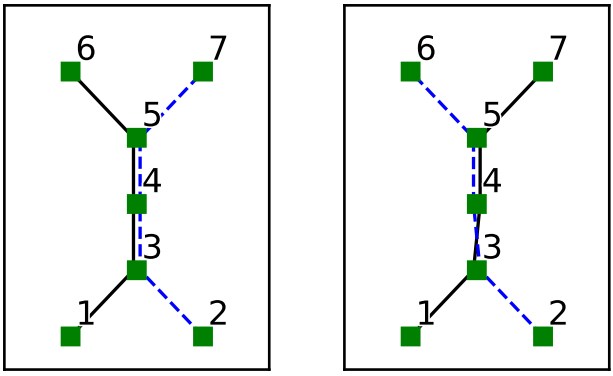

Fig. 2 Illustration of crossing and non-crossing paths

crossing-free. Definition 1 thus excludes all sets of trees that would be excluded simply by disallowing pairs of crossing arcs.

Remark 3 Definition 1 excludes more sets of trees than those mentioned in Remark 2. An example is depicted in Fig. 2. The set consisting of paths $(1, 3, 4, 5, 6)$ and $(2, 3, 4, 5, 7)$ is crossing-free, as their embeddings can be perturbed by an arbitrarily small amount ε such that they have no points in common (see the illustration on the left).

This is not the case for paths $H = (1, 3, 4, 5, 7)$ and $H' = (2, 3, 4, 5, 6)$. When ε is sufficiently small, the perturbed embeddings $F_H(L(H))$ and $F_{H'}\left(L(H')\right)$ have to share at least one point (illustration on the right).

The cable laying optimization problem outlined in Sect. 2.1 can now be stated in formal terms.

Problem 1 Find a set $\mathcal{H}$ of directed subtrees of G satisfying the conditions:

1. the trees cover the turbine nodes, i.e., $T \subset \bigcup_{H\in\mathcal{H}} N(H)$,
2. $|N(H) \cap D| = 1$ for all trees $H \in \mathcal{H}$,
3. $\delta^+_{iH} \leq m$ for all trees $H \in \mathcal{H}$ and all turbine nodes $i \in T \cap N(H)$,
4. $\delta^+_{iH} = 1$ for all trees $H \in \mathcal{H}$ and all obstacle nodes $i \in N(H) \cap O$,
5. $\mathcal{H}$ is crossing-free,

and a function $h : T \mapsto \mathcal{H}$ assigning a unique tree to each turbine node, satisfying the conditions:

1. $t \in N(h(t))$ for all turbine nodes $t \in T$,
2. $|\{t \in T : h(t) = H\}| \leq C$ for all trees $H \in \mathcal{H}$,

such that the total cost $\sum_{H\in\mathcal{H}} \sum_{(i,j)\in A(H)} c(i, j)$ is minimized.

Each tree $H \in \mathcal{H}$ corresponds to a, possibly ramified, cable connecting at most C (condition 2 on h) turbines to a unique (condition 2 on $\mathcal{H}$) substation. The cables cover all turbines in T (condition 1 on $\mathcal{H}$) and branching is allowed up to a maximum branching capacity m at turbine locations (condition 3 on $\mathcal{H}$),while no branching is possible at optional connection points (condition 4 on $\mathcal{H}$). Cable crossing is disallowed by condition 5 on $\mathcal{H}$.

Nodes can possibly be contained in multiple trees in $\mathcal{H}$, reflecting the fact that more than one cable can be present at the same location. To each $t \in T$, the function h allocates a

unique tree $H \in \mathcal{H}$, such that $t \in H$ (condition 1 on h). Which of its present cables a turbine is connected to, is thus given by the function.

3 Integer programming model

In this section, we develop an integer programming model for the problem discussed in Sect. 2. It is an extension of the model presented in the conference publication (Klein et al. 2015). In addition to the features of the earlier model, the current one includes obstacle avoidance and allowance of parallel cables, as explained in Sect. 2.1.

3.1 Basic assumptions

Efficient numerical representations of Problem 1 are not evident. In particular, the non-crossing constraints are challenging, as they involve identification of functions F_H satisfying the conditions in Definition 1. That the range of each F_H can be reduced from a continuous to a *finite* set of points in the plane, which is demonstrated next, is crucial for validity of the integer programming model to follow.

The model is based upon an extension $\widetilde{G}$ of the graph G defined in Sect. 2.2. Added nodes represent possible values of $F_H(L(i))$ for any $H \in \mathcal{H}$ and $i \in N(H)$. Because Condition 2 of Definition 1 implies that $F_H(L(i)) \neq F_{H'}(L(i))$ when $i \in N(H) \cap N(H')$ and $H \neq H'$, the trees in $\widetilde{G}$ corresponding to H and H' have no nodes (besides the root) in common. Consequently, the integer programming model amounts to identifying a *forest* in $\widetilde{G}$. Each tree in this forest corresponds to a maximal subset of trees $H \in \mathcal{H}$ in G with a common root. The integer programming model relies on the following assumption, where $\widetilde{\varepsilon} > 0$ is a model parameter:

Assumption 1 The embedding $L : N \mapsto \mathbb{R}^2$ satisfies $\text{dist}\,(L(j), L(i,k)) > 2\widetilde{\varepsilon}$ for all $i, j, k \in N$, where $i \neq j \neq k \neq i$.

Situations where the end node of an arc is embedded on another arc (Fig. 3 on the left) are avoided by Assumption 1. Further, it is assured that if all functions F_H satisfy condition 1 in Definition 1, for $\varepsilon \leq \widetilde{\varepsilon}$, then the set of crossing arcs is invariant under the transformations F_H. That is, $L(i, j) \cap L(i', j') \neq \varnothing$ if and only if $\left[F_H(L(i)), F_H(L(j))\right] \cap$

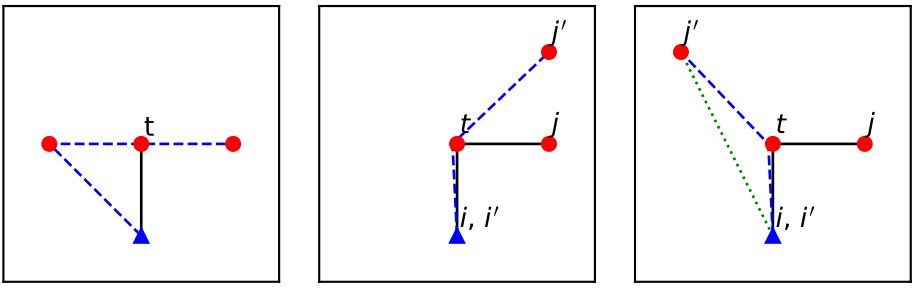

Fig. 3 *Left*: Node embedding of t on arc embedding. *Middle*: Cone of *black cable* is in the cone of *blue dashed cable* at turbine node t. *Right*: *Blue dashed cable* cannot be part of an optimal solution. Cone of *black cable* is not in the cone of *blue dashed cable* at node t. The *green dotted cable* would offer a better solution than the *blue dashed cable*. (Color figure online)

$\left[F_{H'}(L(i')), F_{H'}(L(j'))\right] \neq \varnothing$, where $(i, j) \in A(H)$, $(i', j') \in A(H')$, and i, j, i', j' are distinct nodes.

Consider an optimal solution $(\mathcal{H}, h)$ to Problem 1, where $H, H' \in \mathcal{H}, t \in T \cap N(H) \cap N(H')$, and $h(t) = H \neq H'$. If $(i, t), (t, j) \in A(H)$ and $(i', t), (t, j') \in A(H')$ then $\text{cone}(i, t, j) \subseteq \text{cone}(i', t, j')$. The assertion holds because otherwise, the arc (i', j') could replace arcs $(i', t), (t, j')$ in H' without introducing a crossing. As arc costs satisfy the triangle inequality, feasibility of such a replacement contradicts optimality. Repeating this argument yields (see Fig. 3 in the middle and on the right):

Remark 4 In an optimal solution $(\mathcal{H}, h)$ to Problem 1, where $\{H \in \mathcal{H} : t \in N(H)\} = \left\{H_0, H_1, \ldots, H_p\right\}$ $(t \in T)$, we have $\text{cone}(i_{k-1}, t, j_{k-1}) \subseteq \text{cone}(i_k, t, j_k)$ $(k = 1, \ldots, p)$, where $(i_k, t), (t, j_k) \in A(H_k)$ and $h(t) = H_0$.

To allow for $p+1$ trees $H_0, H_1, \ldots, H_p \in \mathcal{H}$ to contain node $t \in T$, parameter p must be input to the MILP model. Likewise, an upper bound r on the number of trees in an optimal $\mathcal{H}$ containing node $o \in O$ also must be assessed. Thus, it is assumed that p and r are integers satisfying:

Assumption 2 Problem 1 has an optimal solution where $|\{H \in \mathcal{H} : t \in N(H)\}| \leq p + 1$ for all $t \in T$, and $|\{H \in \mathcal{H} : o \in N(H)\}| \leq r + 1$ for all $o \in O$.

3.2 Extended network representation

Based on observations and assumptions stated in the previous section, we introduce the network extension on which the MILP model is built. Two sets of optional nodes, referred to as *Steiner* nodes, are added when developing $\widetilde{G}$ from G.

3.2.1 Steiner nodes surrounding turbine nodes

For each turbine node $t \in T$, we introduce $3p$ Steiner nodes. In each of p orbits centered at $L(t)$, 3 nodes are embedded. More precisely, for $k = 1, \ldots, p$, let $\Gamma_t^k = \left\{\sigma_t^{k1}, \sigma_t^{k2}, \sigma_t^{k3}\right\}$ be a set of nodes with embeddings $L\left(\sigma_t^{k1}\right)$, $L\left(\sigma_t^{k2}\right)$, $L\left(\sigma_t^{k3}\right)$ distributed uniformly on the circle line with radius $\frac{k}{p}\widetilde{\varepsilon}$ centered at $L(t)$. Further, let $L(t), L\left(\sigma_t^{1,1}\right), \ldots, L\left(\sigma_t^{p1}\right)$ be on a joint radial line.

Consider the case where $p = 1$, i.e., Problem 1 has an optimal solution $(\mathcal{H}, h)$ where at most two trees, $H, H' \in \mathcal{H}$, share turbine node $t \in T$. That $F_{H'}$ $(h(t) = H \neq H')$ can be chosen such that $F_{H'}(L(t)) = L(\sigma)$ for some $\sigma \in \Gamma_t^1$ is shown as follows: For $(i', t) \in A(H')$, there exist a $\sigma_{i'} \in \Gamma_t^1$ and a closed half-plane $\mathcal{P}_{i'} \subset \mathbb{R}^2$ such that $L(i', \sigma_{i'}) \subset \partial\mathcal{P}_{i'}$, $L(t) \notin \mathcal{P}_{i'}$, and $\mathcal{P}_{i'} \cap \left\{L\left(\sigma_t^{1,1}\right), L\left(\sigma_t^{1,2}\right), L\left(\sigma_t^{1,3}\right)\right\} = L(\sigma_{i'})$. Thus, there is no arc in any tree in $\mathcal{H}$ with embedding partly inside and partly outside of $\mathcal{P}_{i'}$. Likewise, for $(t, j') \in A(H')$, there exist a $\sigma_{j'} \in \Gamma_t^1$ and a closed half-plane $\mathcal{P}_{j'} \subset \mathbb{R}^2$ with analogous properties. Consequently, if $\sigma_{i'} \neq \sigma_{j'}$, $L\left(\sigma_{i'}, \sigma_{j'}\right)$ does not intersect the embedding of any arc of trees in $\mathcal{H}$. An illustration is given in Fig. 4.

For $p > 1$, Remark 4 shows that the arguments above can be applied sequentially to $H_1, \ldots, H_p$. Let $(i_k, t), (t, j_k) \in A(H_k)$ $(k = 0, 1, \ldots, p)$. Due to the embedding of $\Gamma_t = \Gamma_t^1 \cup \cdots \cup \Gamma_t^p$ in orbits around $L(t)$, there exist Steiner nodes $\sigma_{i_k}, \sigma_{j_k} \in \Gamma_t^k$, with corresponding half-planes $\mathcal{P}_{i_k}$ and $\mathcal{P}_{j_k}$ such that $L(i_k, \sigma_{i_k}) \subset \partial\mathcal{P}_{i_k}$, $L(t) \cap \left\{L(\sigma) : \sigma \in \Gamma_t^1 \cup \cdots \cup \Gamma_t^{k-1}\right\} \cap \mathcal{P}_{i_k} = \varnothing$, and $\mathcal{P}_{i_k} \cap \left\{L\left(\sigma_t^{k1}\right), L\left(\sigma_t^{k2}\right), L\left(\sigma_t^{k3}\right)\right\} = L(\sigma_{i_k})$, and analogous conditions fulfilled by σ_{j_k} and $\mathcal{P}_{j_k}$.

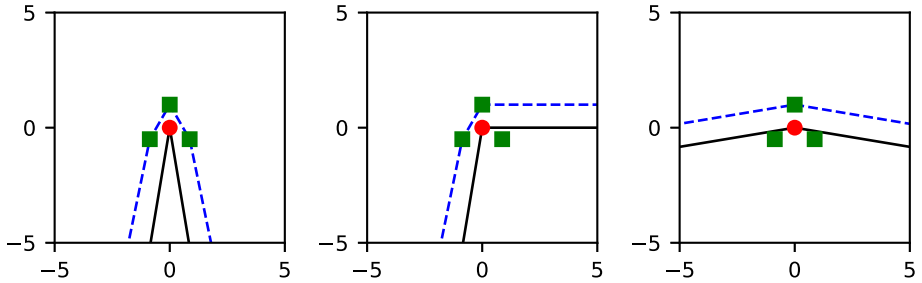

Fig. 4 The three possible cases of Steiner nodes in Γ_t^1 used for laying a cable around turbine t. *Green squares* are Steiner nodes, *red circles* are turbine nodes. (Color figure online)

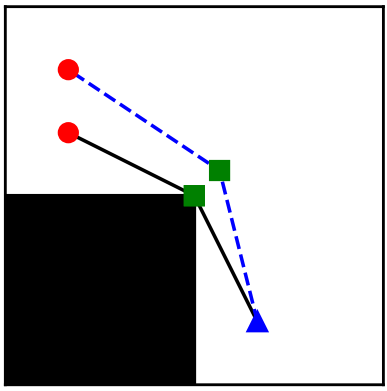

Fig. 5 Example of cables around obstacle (*black area*). *Green squares* are Steiner points at obstacle corners, *red circles* are turbines, *blue triangle* is substation. (Color figure online)

3.2.2 Steiner nodes surrounding obstacle nodes

We introduce r Steiner nodes for each obstacle node $o \in O$. Let $\Gamma_o = \{\rho_o^0, \rho_o^1, \ldots, \rho_o^r\}$, where $\rho_o^0 = o$, be a set of nodes embedded uniformly along a straight line intersecting $L(o)$. More precisely, consider the convex polygonal obstacle Ω of which $L(o)$ is a vertex, and let $\mathcal{L}$ denote the angle bisector of the two neighbouring vertices in Ω at $L(o)$. We choose the embedding such that $L\left(\rho_o^1\right), \ldots, L\left(\rho_s^r\right) \in \mathcal{L} \setminus \Omega$, and such that $\left\|L\left(\rho_o^k\right) - L(o)\right\|_2 = \frac{k}{r}\widetilde{\varepsilon}$ $(k = 1, \ldots, r)$.

If $r = 0$, it is assumed that it is optimal to lay at most one cable around each obstacle. If $r > 0$, we can have $o \in O \cap N(H_0) \cap \cdots \cap N(H_r)$, for distinct $H_0, \ldots, H_r \in \mathcal{H}$. As Ω is convex, an observation analogous to Remark 4 for turbine nodes t can be made for an obstacle node o. However, only one of the Steiner nodes $\rho_o^0, \ldots, \rho_o^r$ is selected for each tree $H_0, \ldots, H_r$ (see Fig. 5).

3.2.3 Network definition

Summarizing Sects. 3.2.1–3.2.2, the node set $\widetilde{N} = D \cup T \cup S$ of the extended graph $\widetilde{G}$ is composed of a set of substation nodes D, mandatory turbine nodes T and a set of optional Steiner nodes $S = \bigcup_{u \in T \cup O} \Gamma_u$.

The arc set $\widetilde{A}$ of $\widetilde{G}$ is defined such that $(i, j) \in \widetilde{A}$ if and only if $(i, j) \in \widetilde{N} \times \widetilde{N}$ satisfies at least one of the conditions:

- $(i, j) \in A$ (thus $\widetilde{A} \supseteq A$),
- $i \in N$, $j \in \Gamma_v$ for some $v \in T \cup O$, and $(i, v) \in A$,
- $i \in \Gamma_u$ for some $u \in T \cup O$, $j \in N$, and $(u, j) \in A$,
- $i \in \Gamma_u$ for some $u \in T \cup O$, $j \in \Gamma_v$ for some $v \in T \cup O$, and $(u, v) \in A$.

We let $\widetilde{N}_i^-$ and $\widetilde{N}_i^+$ denote the set of in-neighbors and the set of out-neighbors, respectively, of node $i \in \widetilde{N}$ in $\widetilde{G}$.

The definition of the arc cost $c(i, j)$ is extended to all $(i, j) \in \widetilde{A}$. The set $\chi \subseteq \widetilde{A} \times \widetilde{A}$ of pairs of crossing arcs is defined as

$$\chi = \left\{ \left((i, j), (i', j')\right) \in \widetilde{A} \times \widetilde{A} : L(i, j) \cap L(i', j') \setminus \left\{ L(i), L(j), L(i'), L(j') \right\} \neq \varnothing \right\}.$$

Problem 1 is now transformed to the problem of finding a minimum cost forest $\mathcal{F} = \left(\widetilde{N}(\mathcal{F}), \widetilde{A}(\mathcal{F})\right) \subseteq \widetilde{G}$, such that $\mathcal{F}$ spans T, and such that no pairs of arcs cross each other. An integer programming formulation of the transformed problem is developed next.

3.3 Model formulation

Recall that all trees in the forest spanning T have leaves only in T and root in D, and that the directed paths are directed from the leaves towards the root. An arc $(i, j) \in \widetilde{A}(\mathcal{F})$ is said to have *load* equal to the number of turbine nodes in the subtree rooted at node i (e.g. all leaves in $\mathcal{F}$ have unit load). Consequently, while traversing a path towards the substation, the load increases by at least 1 at every turbine node, whereas it might remain unchanged at Steiner nodes.

For each $(i, j) \in \widetilde{A}$, we define the binary variable y_{ij}, indicating whether or not $(i, j) \in \widetilde{A}(\mathcal{F})$. For each $k = 1, \ldots, C$, we introduce the binary variable z_{ij}^k indicating whether or not $(i, j) \in \widetilde{A}(\mathcal{F})$ with load k. Since no arc entering some $j \in T$ can have load C, we let $z_{ij}^C = 0$ be a constant for all $i \in \widetilde{N}_j^-$. Because $y_{ij} = \sum_{k=1}^C z_{ij}^k$, the y-variables can be eliminated, but for convenience, they are kept in the formulation below.

We arrive at the following model formulation:

$$\min_{y,z} \quad \sum_{(i,j)\in\widetilde{A}} c(i, j) y_{ij}, \tag{1}$$

$$\sum_{h=1}^C z_{ij}^h = y_{ij}, \qquad (i, j) \in \widetilde{A}, \tag{2}$$

$$\sum_{j\in\widetilde{N}_i^+} y_{ij} = 1, \qquad i \in T, \tag{3}$$

$$\sum_{j\in\widetilde{N}_i^+} y_{ij} \leq 1, \qquad i \in S, \tag{4}$$

$$\sum_{h=1}^C h \left(\sum_{j\in\widetilde{N}_i^+} z_{ij}^h - \sum_{j\in\widetilde{N}_i^-} z_{ij}^h \right) = 1, \quad i \in T, \tag{5}$$

$$\sum_{j\in\widetilde{N}_i^+} z_{ij}^k - \sum_{j\in\widetilde{N}_i^-} z_{ji}^k = 0, \qquad i \in S; k = 1, \ldots, C, \tag{6}$$

$$\sum_{j\in\widetilde{N}_i^-} y_{ji} \leq m, \qquad i \in T, \tag{7}$$

$$y_{ij} + y_{i'j'} \leq 1, \qquad \left((i, j), (i', j')\right) \in \chi, \tag{8}$$

$$\sum_{i\in\Gamma_t^k} \sum_{j\in\widetilde{N}_i^+\setminus\Gamma_t^k} y_{ij} \leq 1, \qquad t \in T, k = 1, \ldots, p, \tag{9}$$

$$z_{ij}^h \in \{0, 1\}, \qquad (i, j) \in \widetilde{A}, h = 1, \ldots, C, \tag{10}$$

$$y_{ij} \in \{0, 1\}, \qquad (i, j) \in \widetilde{A}. \tag{11}$$

We minimize the total cable cost in the objective function (1). Constraint (3) assures that each turbine node has exactly one outgoing arc, while (4) implies Steiner nodes have zero or

Table 1 Information on the examined wind farms

Wind farm	Number of turbines	Number of substations
Barrow	30	1
Walney 1	51	1
Walney 2	51	1
Sheringham Shoal	88	2

one outgoing arc. By Eq. (5), the load of the arc leaving turbine node j equals one more than the sum of the loads of entering arcs. Likewise, constraint (6) ensures that each Steiner node has an outgoing arc with load k if and only if it has an entering arc with that load. By (7), the number of branches at a turbine node is no more than the branching capacity m. Finally, avoidance of crossing arcs is ensured by constraint (8).

4 Numerical experiments

4.1 Wind park data

In the numerical experiments, turbine location data of the offshore wind farms Barrow, Walney 1, Walney 2 and Sheringham Shoal are used as input to the model in Sect. 3.3. A tabular overview of the number of turbines and substations can be seen in Table 1. All input data are publicly available (KIS-ORCA 2017).

The available positional data have an accuracy of one meter. We choose $\widetilde{\varepsilon} = 0.0005$ meters (see Sect. 3.1), and perturb the turbine positions by up to one meter, within the accuracy of the positional data, such that Assumption 1 is satisfied in all instances.

There are no obstacles in the wind farms Barrow, Walney 1 and Sheringham Shoal. The Walney 2 wind farm has a subsea cable crossing between the upper and lower section of turbines, and it is desirable to cross this cable only at one location. We thus place two obstacles along the subsea cable, with a small opening in between. Model (1)–(11), defined for the graph $\widetilde{G}$ containing Steiner nodes, makes it possible to find feasible solutions. Without the Steiner nodes embedded at the obstacle corners, no feasible solution can be found, as the direct paths between the turbines in this section of Walney 2 and the substation and other turbines are blocked by the obstacles.

4.2 Implementation

The model presented in the previous section is implemented by using the CPLEX 12.3 Python 3.4 API. This enables use of the branch-and-cut callback functions of CPLEX for dynamic constraint generation, which is useful for handling the non-crossing constraints (8). Because the number $|\chi|$ of such constraints is too large, it is practically infeasible to include all constraints (8) from the start of the optimization process.

Instead, we implement a CPLEX lazy constraint callback function which allows adding constraints iteratively, while the problem is being solved by branch-and-cut search. Within the callback function, the variable values of the current solution are available. This allows adding only violated non-crossing constraints (8). CPLEX guarantees that all constraints added in this way are satisfied in the final solution.

The constraint generation scheme ensures that only a small fraction of the total number of non-crossing constraints is added to the model during the solution process. For example, the Barrow wind farm with $|N| = 31$ has about 1 million non-crossing constraints (8). However, in most instances, the number of added non-crossing constraints is below 100.

All experiments are carried out on a Intel Xenon E5-2699 CPU with 72 logical cores and 256 GB of RAM. The corresponding CPLEX options are set to `parallel` $= 1$ and `threads` $= 70$.

All feasible instances are solved to optimality, except for Sheringham Shoal with $C = 6$ and $p = 1$. We do not give a detailed report of the execution time, as the machine used for the numerical experiments is usually under heavy load, and thus the execution times are not reproducible, but most instances are solved to optimality in 1–10 min. Notable exceptions are the Walney 2 and Barrow wind farm instances with cable capacity $C = 5$, which require an execution time between 1 and 2 h. In the Sheringham Shoal instance with $C = 6$ and $p = 1$, the solver stopped after 4 days of runtime with an optimality gap of 0.65% due to excessive memory usage (280 GB tree size).

4.3 Numerical results

Numerical experiments on the wind farms listed above are conducted, varying the cable capacity C and the number p (see Sect. 3.2.1) of Steiner node orbits per turbine. The purpose of the experiments is to investigate what cost reductions that can be obtained by allowing parallel cables, as well as cables around turbines. To that end, we compare the minimum cost in (1)–(11) for positive values of p to the reference case $p = 0$. For the wind farm instances without obstacles, the reference case implies an instance of $\widetilde{G}$ without Steiner nodes ($S = \varnothing$).

The number r of Steiner nodes surrounding each obstacle node $o \in O$ (see Sect. 3.2.2) in the Walney 2 instance is set to $r = 3$. Because $|O| = 2$ in this instance, and $|\Gamma_o| = r + 1$ for each $o \in O$, $r = 3$ results in a total of 8 Steiner nodes (including the obstacle nodes O) in the gap between the two obstacles. This is sufficient for connecting all 15 turbines separated by the obstacles for $C \geq 2$. Choosing r smaller makes the model instance infeasible for small C.

The branching capacity is limited to $m = 3$ in all experiments. The cost coefficients $c(i, j)$ have been chosen to be the Euclidean distance $\|L(i) - L(j)\|_2$ between the node embeddings.

For faster computations, only arcs with Euclidean length no more than a given bound are kept in the arc set $\widetilde{A}$ in the numerical calculations. Arcs $(i, j) \in \widetilde{A}$ for which $c(i, j) \geq d_{\max}$, where $d_{\max}$ is a model parameter referred to as the *cut-off length*, are eliminated from $\widetilde{A}$. In order to select an appropriate cut-off length $d_{\max}$, we conduct a series of experiments with cable capacity $C = 2$ and $p = 0$ with varying values for $d_{\max}$. The results are listed in Table 2. Choosing $d_{\max} = 4000$ results in the same minimum cost as the one obtained with no limitation on the maximum arc length. This is true in all wind farm instances but Walney 2, in which case $d_{\max} = 5000$ is necessary in order to avoid an increased cost. We thus select these values of $d_{\max}$ in the following experiments of the respective wind farms.

In a second set of experiments, we investigate how cable costs can be reduced by different values of C and p. Numerical experiments on the Barrow instance show that the results with $p = 2$ are equal to those obtained for $p = 1$ for $C = 1, \ldots, 5$. We thus limit the investigation of the other wind farms to $p = 0$ and $p = 1$.

The results of these numerical experiments are given in Table 3. Small reductions in the minimum cost in the range of 0.5–1% are seen for values of C up to 5. The turbine and

Table 2 Optimal values for different choices of $d_{\max}$ when $C = 2$ and $p = 0$

$d_{\max}$	Barrow	Walney 1	Walney 2	Sheringham Shoal
2000	*	*	*	*
3000	38,093	72,640	105,998	102,032
4000	37,802	70,734	100,354	100,284
5000	37,802	70,734	98,924	100,284
6000	37,802	70,734	98,924	100,284
Unlimited	37,802	70,734	98,924	100,284

Asterisks (*) signify infeasible instances

Table 3 Optimal values for different choices of C and p

C	p	Barrow	Walney 1	Walney 2	Sheringham Shoal
2	0	37,802	70,734	98,924	100,284
2	1	36,990	70,286	97,885	99,865
3	0	27,980	55,518	74,711	78,187
3	1	27,773	55,107	74,302	78,187
4	0	23,567	47,652	63,571	68,938
4	1	23,208	47,411	63,496	68,862
5	0	20,737	43,420	56,904	64,362
5	1	20,691	43,420	56,904	64,362
6	0	18,375	41,418	52,981	61,463
6	1	18,374	41,418	52,981	61,463*

*0.64% optimality gap

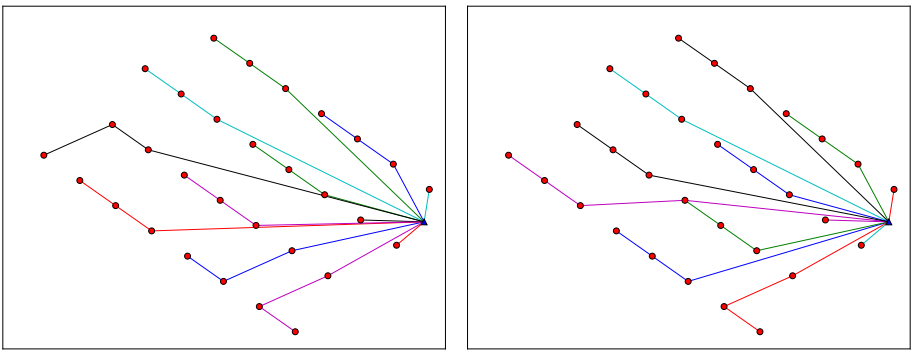

Fig. 6 Optimal cable layout of Barrow wind farm with $C = 3$ and $p = 0$ (*left*), and $p = 1$ (*right*)

substation layout seems to have a significant effect on the cost reductions achievable by allowing cabling around other turbines. It is noticeable that reductions up to $C = 5$ can only be observed in the Barrow instance. Unlike the other wind farms, where the substations are located near the geographical center, the substation of Barrow is positioned on the side of the turbines. Illustrations of two solutions for Barrow and one solution for Walney 2 are given in Figs. 6 and 7, respectively.

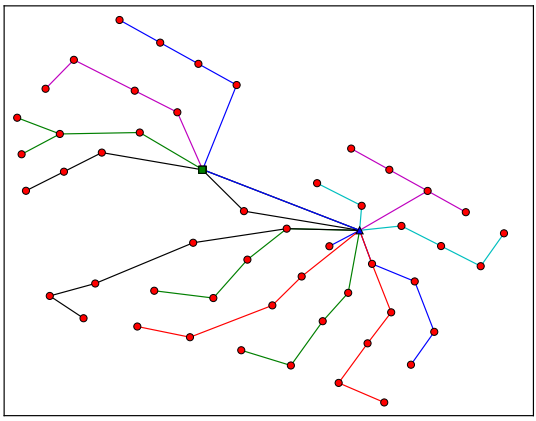

Fig. 7 Optimal cable layout of Walney 2 with $C = 4$, $r = 4$ and $p = 1$

5 Conclusion

The most significant achievement from the introduction of the model featuring Steiner nodes, is its ability to find optimal solutions to problem instances including obstacles. With obstacles allowing only a narrow cable path as in Walney 2, no feasible solutions would exist otherwise.

The additional Steiner nodes surrounding the turbine locations, which allow for parallel cables and cables around turbines, contribute to small cost reductions in the optimal solutions. The exact amount of the reductions depend heavily on the turbine layout and the cable capacity. As expected, these cost reductions are in general smaller than those achieved by the introduction of branching (Klein et al. 2015), but can still be considerable taking into account the high cost per meter of cables in offshore wind farms. A surprising result is that the Steiner nodes around turbine locations are not used in the instances with higher cable capacities. It is likely that this is a consequence of the regular layouts of the wind farms, in combination with absence of obstacles. To study this more closely, an examination of more irregular turbine layouts, possibly including fine-grained obstacle data, should be undertaken.

Small adjustments to the model formulated in the current work allow for instance specific customization. In cases like Walney 2, it is relevant to optimize the unique location at which the turbine power cables should cross the already existing subsea cable. This is accomplished by introducing several mutually exclusive groups of Steiner nodes, one group for each feasible crossing location, connecting the two parts of the wind farm.

In this article, one MILP model for the cable layout problem under study has been developed. Fortunately, the model produces interesting results in realistic wind farm instances, and proves to have a computational performance that makes it practical and applicable. It will, however, be a challenge to adopt the model and algorithm such that it can handle large scale wind farms in the future, with possibly 200 or more turbines. Alternative model formulations, and comparisons of their computational properties, have not been an issue in the current work. This is left as a challenging topic for future research.

References

Bauer, J., & Lysgaard, J. (2015). Offshore wind farm array cable layout problem. *Journal of the Operational Research Society*, *66*(3), 360–368.

Cerveira, A., de Sousa, A., Pires, E. J. S., & Baptista, J. (2016). Optimal cable design of wind farms: The infrastructure and losses cost minimization case. *IEEE Transactions on Power Systems*, *31*(6), 4319–4329.

DONG Energy Hornsea Project One (UK) Ltd. (2017). Hornsea project one. http://www.hornseaprojectone.co.uk. Accessed 10 June 2017.

Fischetti, M., & Pisinger, D. (2016). Inter-array cable routing optimization for big wind parks with obstacles. In *Control Conference (ECC), 2016 European* (pp. 617–622). IEEE.

Foley, A. M., Leahy, P. G., Marvuglia, A., & McKeogh, E. J. (2012). Current methods and advances in forecasting of wind power generation. *Renewable Energy, 37*(1):1–8. ISSN 09601481.

Gonzalez-Longatt, F. M., Wall, P., Regulski, P., & Terzija, V. (2012). Optimal electric network design for a large offshore wind farm based on a modified genetic algorithm approach. *IEEE Systems Journal*, *6*(1), 164–172.

Greater Gabbard Offshore Winds Ltd. (2005). Greater gabbard offshore windfarm: Non-technical summary.http://sse.com/media/93004/NonTechnicalSummary.pdf. Accessed 27 June 2017.

GWEC. (2015). Global wind energy council: Global wind report 2013. http://www.gwec.org. Accessed 01 Dec 2015.

Hertz, A., Marcotte, O., Mdimagh, A., Carreau, M., & Welt, F. (2017). Design of a wind farm collection network when several cable types are available. *Journal of the Operational Research Society*, *68*(1), 62–73.

Hou, P., Hu, W., Chen, C., & Chen, Z. (2016). Optimisation of offshore wind farm cable connection layout considering levelised production cost using dynamic minimum spanning tree algorithm. *IET Renewable Power Generation*, *10*(2), 175–183.

Hwang, F. K., Richards, D. S., & Winter, P. (1992). *The Steiner tree problem. Annals of discrete mathematics* (Vol. 53). North Holland: Elsevier. ISBN 9780444890986.

Irawan, C.A., Ouelhadj, D., Jones, D., Stlhane, M., & Sperstad, I. B. (2017). Optimisation of maintenance routing and scheduling for offshore wind farms. *European Journal of Operational Research, 256*(1), 76–89. ISSN 0377-2217.

KIS-ORCA. (2017). Kingfisher awareness charts. http://www.kis-orca.eu. Accessed 10 Jan 2017.

Klein, A., Haugland, D., Bauer, J., & Mommer, M. (2015). An integer programming model for branching cable layouts in offshore wind farms. *Advances in Intelligent Systems and Computing*, *359*, 27–36.

Lingling, H., Yang, F., & Xiaoming, G. (2009). Optimization of electrical connection scheme for large offshore wind farm with genetic algorithm. In *International Conference on Sustainable Power Generation and Supply, 2009* (pp. 1–4).

London Array Limited. (2017). London array, the worlds largest offshore wind farm. http://www.londonarray.com. Accessed 10 June 2017.

Pillai, A. C., Chick, J., Johanning, L., Khorasanchi, M., & de Laleu, V. (2015). Offshore wind farm electrical cable layout optimization. *Engineering Optimization*, *47*(12), 1689–1708.

Réthoré, P. -E., Fuglsang, P., Larsen, G. C., Buhl, T., Larsen, T. J., & Madsen., H. A. (2014). TOPFARM: Multi-fidelity optimization of wind farms. *Wind Energy, 17*(12):1797–1816. ISSN 10954244.

Wdzik, A., Siewierski, T., & Szypowski, M. (2016). A new method for simultaneous optimizing of wind farms network layout and cable cross-sections by MILP optimization. *Applied Energy*, *182*, 525–538.

WindEurope. (2017). The European offshore wind industry: Key trends and statistics 2016. http://windeurope.org. Accessed 05 Jan 2017.